Journal of Neuroscience Research 85:3294–3303 (2007)

On the Reliability of ^{13}C Metabolic Modeling With Two-Compartment Neuronal-Glial Models

Alexander A. Shestov, Julien Valette, Kâmil Uğurbil, and Pierre-Gilles Henry*

Center for Magnetic Resonance Research, University of Minnesota, Minneapolis, Minnesota

Metabolic modeling of ^{13}C NMR spectroscopy (^{13}C MRS) data using two-compartment neuronal-glial models enabled non-invasive measurements of the glutamate-glutamine cycle rate (V_{NT}) in the brain in vivo. However, the reliability of such two-compartment metabolic modeling has not been examined thoroughly. This study uses Monte-Carlo simulations to investigate the reliability of metabolic modeling of ^{13}C positional enrichment time courses measured in brain amino acids such as glutamate and glutamine during [1-^{13}C]- or [1,6-$^{13}C_2$]glucose infusion. Results show that the determination of V_{NT} is not very precise under experimental conditions typical of in vivo NMR studies, whereas the neuronal TCA cycle rate $V_{TCA(N)}$ is determined with a much higher precision. Consistent with these results, simulated ^{13}C positional enrichment curves for glutamate and glutamine are much more sensitive to the value of $V_{TCA(N)}$ than to the value of V_{NT}. We conclude that the determination of the glutamate-glutamine cycle rate V_{NT} using ^{13}C MRS is relatively unreliable when fitting ^{13}C positional enrichment curves obtained during [1-^{13}C] or [1,6-$^{13}C_2$]glucose infusion. Further developments are needed to improve the determination of V_{NT} , for example using additional information from ^{13}C-^{13}C isotopomers and/or using glial specific substrates such as [2-^{13}C]acetate.

Key words: metabolic modeling; ^{13}C; magnetic resonance spectroscopy; neuronal-glial compartmentation; glutamate-glutamine cycle

Carbon-13 NMR spectroscopy (^{13}C MRS) is a unique tool to measure metabolic fluxes non-invasively in the brain (Gruetter, 2002; Henry et al., 2006). NMR measurements during infusion of a ^{13}C-label substrate (e.g., [1-^{13}C]glucose) enables detection of time courses of ^{13}C label incorporation into brain amino acids such as glutamate, glutamine, and aspartate (de Graaf et al., 2003b; Gruetter et al., 2003a). Analysis of these ^{13}C time courses using metabolic models has the potential to yield quantitative metabolic fluxes such as the rate of TCA cycle or the rate of glutamate-glutamine cycle between neurons and astrocytes (Rothman et al., 2003; Garcia-Espinosa et al., 2004; Shen, 2006).

Metabolic modeling was carried out initially using single-compartment models to fit glutamate turnover curves (Chance et al., 1983; Mason et al., 1992, 1995). Because most glutamate is located in neurons (Ottersen et al., 1992), such one-compartment models reflect mostly neuronal metabolism. These experiments permitted measurement of the neuronal TCA cycle flux as well as the exchange flux V_X between 2-oxoglutarate and glutamate (Mason et al., 1992, 1995; Henry et al., 2002). In the 1990s, glutamine became measurable also by NMR (Gruetter et al., 1994), and models were developed to fit not only glutamate but also glutamine turnover curves. This led to the landmark proposal that the glutamate–glutamine cycle between neurons and astrocytes could be measured in vivo (Sibson et al., 1997). Initial two-compartment models did not include a full astrocytic compartment, but expanded models were proposed soon afterward to include astrocytic TCA cycle activity and pyruvate carboxylase activity in glia (Gruetter et al., 1998, 2001; Shen et al., 1999). Even more complex models have been proposed recently to measure not only the glutamate–glutamine cycle, but also the GABA-glutamine cycle (Patel et al., 2005). Surprisingly, however, the precision with which metabolic fluxes can be measured using such complex metabolic models has not been examined thoroughly.

Abbreviations used: AspC23, average of aspartate C2 and aspartate C3; A, astrocytic; BFGS algorithm, Broyden-Fletcher-Goldfarb-Shanno algorithm; Glu, glutamate; Gln, glutamine; Glx, sum of glutamate and glutamine; Lac, lactate; MRS, magnetic resonance spectroscopy; N, neuronal; OAA, oxaloacetate; Pyr, pyruvate; TCA cycle, tricarboxylic acid cycle; 2OG, 2-oxoglutarate; V_{NT}, rate of glutamate-glutamine cycle; $V_{TCA(N)}$, rate of neuronal TCA cycle; $V_{TCA(A)}$, rate of astrocytic TCA cycle; V_{PC}, rate of pyruvate carboxylase; V_X, rate of exchange between 2-oxoglutarate and glutamate; V_{OUT}, rate of lactate dilution.

Contract grant sponsor: NIH; Contract grant numbers: R01NS38672, P41RR08079, P30NS057091; Contract grant sponsors: Keck Foundation, MIND institute.

*Correspondence to: Pierre-Gilles Henry, Center for Magnetic Resonance Research, 2021 6th St SE, Minneapolis MN 55455.
E-mail: henry@cmrr.umn.edu

Received 8 November 2006; Revised 10 December 2006, 18 December 2006; Accepted 9 January 2007

Published online 28 March 2007 in Wiley InterScience (www.interscience.wiley.com). DOI: 10.1002/jnr.21269

The objective of this study was to investigate the reliability of existing two-compartment neuronal-glial models used to determine metabolic fluxes from ^{13}C MRS data. Nearly all metabolic modeling studies with two-compartment models have been carried out using [1-^{13}C]glucose or [1,6-$^{13}C_2$]glucose as a substrate. The measured turnover curves used for the fitting typically correspond to the total ^{13}C enrichment at each carbon position (positional ^{13}C enrichment) such as the C4, C3, C2 positions of glutamate and glutamine. We focused our simulations on the use of two-compartment models to fit positional ^{13}C enrichment curves obtained during [1-^{13}C]glucose or [1,6-$^{13}C_2$]glucose infusion. We carried out Monte-Carlo simulations under different simulated experimental conditions, varying parameters such as the number of experimental data points per turnover curve, the number of fitted turnover curves, or the noise level. In addition, we studied the sensitivity of turnover curves to changes in the value of specific metabolic fluxes. This allowed us to determine the reliability of each fitted metabolic flux in the model depending on simulated experimental conditions.

MATERIALS AND METHODS

All simulations were carried out in Matlab (The MathWorks Inc., Matick, MA) using a two-compartment model similar to those already published (Gruetter et al., 1998, 2001; Shen et al., 1999). The actual metabolic model used for this study is essentially identical to (Gruetter et al., 2001) and is shown in Figure 1. Metabolic fluxes were assumed as follows (in μmol g^{-1} min^{-1}): $V_{TCA(N)} = 1$, $V_{TCA(A)} = 0.1$, $V_{NT} = 0.3$, $V_{PC} = 0.1$, $V_X = 1$, $V_{OUT} = 0.3$ (see Fig. 1 for a definition of these metabolic fluxes). These values are representative of metabolic fluxes in the resting human brain or in the anesthetized rat brain. Metabolite concentrations were assumed as follows: $[GLU]_N = 9$ mM, $[GLU]_A = 1$ mM, $[GLN]_N = 0.4$ mM, $[GLN]_A = 3.6$ mM, [Lac] = 1.0 mM, $[Asp]_N = 2.0$ mM, and $[OAA]_N = [OAA]_A = [2OG]_N = [2OG]_A = 0.1$ mM.

The metabolic model consists of 25 differential equations (Gruetter et al., 2001). This system of coupled differential equations was solved numerically using a fourth order Runge Kutta method for stiff systems. Solving differential equations yields positional ^{13}C enrichment curves for glutamate C4, C3, C2, glutamine C4, C3, C2, and AspC23 (average of aspartate C2 and aspartate C3) during an infusion of [1-^{13}C] or [1,6-$^{13}C_2$]glucose. All simulations reported in the present study were carried out assuming [1-^{13}C]glucose infusion (using [1,6-$^{13}C_2$]glucose infusion leads to approximately two-fold higher signal-to-noise ratio due to the generation of two molecules of [3-^{13}C]pyruvate instead of one).

The Monte-Carlo simulation procedure was carried out as follows: synthetic turnover curves for Glu C4, C3, C2, glutamine C4, C3, C2, and AspC23 were generated by solving differential equations and adding Gaussian white noise with mean zero and standard deviation (SD) σ. These synthetic turnover curves were characterized by the following parameters: number of points per curve, noise level (σ) and total duration of time courses (t_{max}). Figure 2 shows an example of such synthetic turnover curves with 40 data points, $t_{max} = 160$ min and a noise level σ = 0.1 μmol g^{-1} that is a typical noise level for in vivo ^{13}C NMR studies.

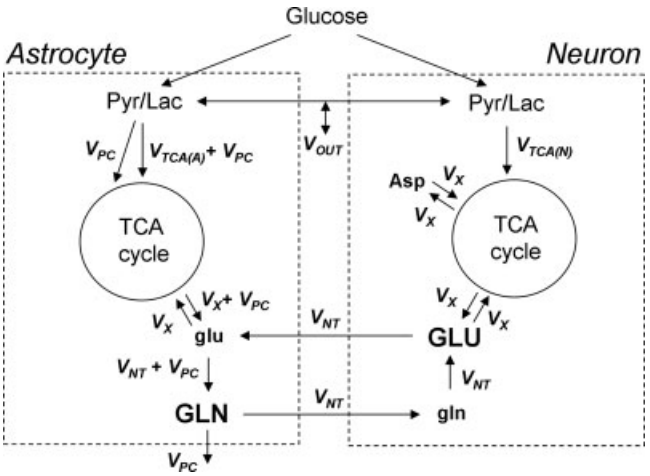

Fig. 1. Two-compartment metabolic model used for Monte-Carlo simulations in the present study. This metabolic model comprises six free parameters: $V_{TCA(N)}$ (neuronal TCA cycle), $V_{TCA(A)}$ (glial TCA cycle), V_{NT} (glutamate-glutamine cycle), V_X (exchange between 2-oxoglutarate and glutamate), V_{PC} (rate of pyruvate carboxylase), and V_{OUT} (lactate dilution flux). Glucose is taken up both by neurons and astrocytes and is oxidized through the TCA cycle in both cell types. The anaplerotic enzyme pyruvate carboxylase (PC) is specific of the glial compartment. The total PDH flux in astrocytes is the sum of $V_{TCA(A)}$ and V_{PC}. Glutamate is linked to the TCA cycle through exchange (V_X) with the TCA cycle intermediate 2-oxoglutarate. On glutamatergic neurotransmission, glutamate is released by presynaptic neurons, taken up by astrocytes, converted to glutamine through the astrocytic enzyme glutamine synthetase (GS) and sent back to neurons to regenerate glutamate. Aspartate is assumed to be located in neurons only, and V_X also represents the exchange rate between oxaloacetate and aspartate. See Gruetter et al. (2001) for additional details on this metabolic model.

These synthetic turnover curves were then fitted using the metabolic model shown on Figure 1 to obtain best fit values for each of the six free parameters $V_{TCA(N)}$, $V_{TCA(A)}$, V_{PC}, V_{NT}, V_X, and V_{OUT}. Minimization was carried out using either the Broyden-Fletcher-Goldfarb-Shanno (BFGS) algorithm or the Simplex algorithm. The BFGS algorithm was faster, and Simplex was used when the BFGS algorithm failed. Different starting values for the fit were chosen randomly around the true (nominal) value of metabolic fluxes parameters to ensure that the results of the simulation were not dependent on the initial conditions of the fit. The fit was repeated at least 500 times with a different noise realization (but the same noise level σ), so that a distribution of fitted values was obtained for each of the six free parameters (Fig. 2 shows an example of distribution obtained for V_{NT} after carrying out 500 fits). Because noise realization is the only variable that differs from one fit to the next, such distributions directly reflect the uncertainty on each fitted parameter under the specific experimental conditions used in the simulation. Distributions were characterized by their SD σ. Other output statistics (not

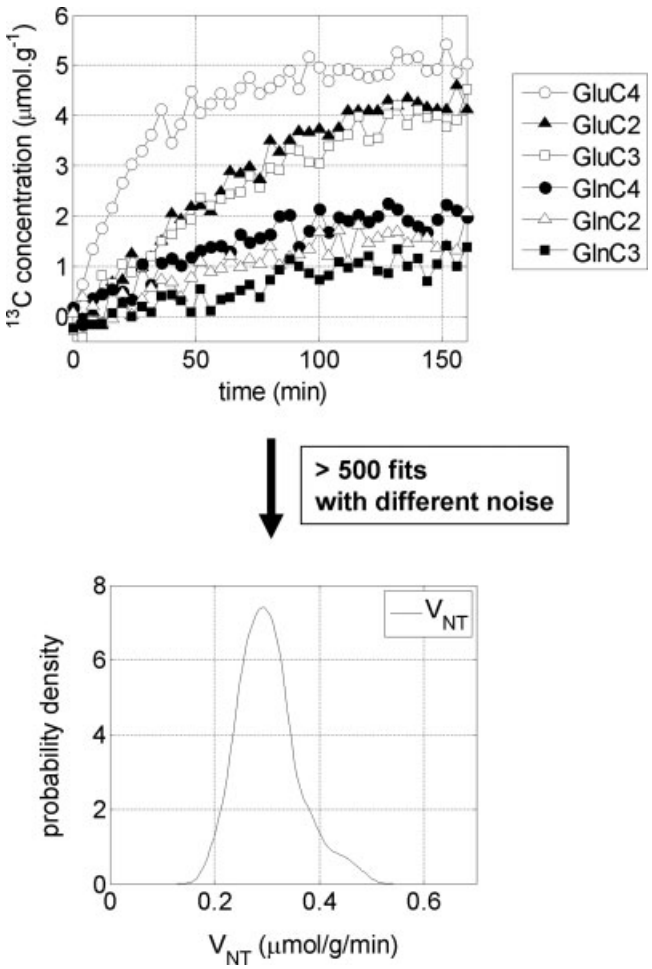

Fig. 2. Schematic description of the Monte-Carlo simulation procedure. "Synthetic" ^{13}C turnover curves are generated by solving the differential equations describing the model with nominal values of metabolic fluxes, and adding gaussian white noise. As an example, the six ^{13}C turnover curves shown here (**top**) were simulated for Glu C4, C3, C2 and glutamine C4, C3, C2 with t_{max} = 160 min, 40 data points per curve, and a noise SD σ = 0.1 μmol g^{-1}, during an infusion of [1,6-$^{13}C_2$]glucose. This ^{13}C turnover curves are then fitted with the metabolic model to obtain the value of the six free parameters for this particular dataset. The procedure is then repeated at least 500 times, and a probability distribution is obtained for each free parameter in the model. An example of probability distribution is shown for V_{NT} (**bottom**). Nominal values for the six free parameters were chosen as follows (in μmol g^{-1} min^{-1}): $V_{TCA(N)}$ = 1, V_{NT} = 0.3, $V_{TCA(A)}$ = 0.1, V_X = 1, V_{PC} = 0.1, V_{OUT} = 0.3. These values are representative of the awake human brain and α-chloralose anesthetized rat brain.

reported here) include confidence intervals (CI) (useful in the case of asymmetric distributions), probability density functions and cross-correlation between free metabolic parameters.

RESULTS

Monte-Carlo simulations were carried out while varying one experimental parameter at a time: the number of data points per curve (keeping the total duration t_{max} constant) (Fig. 3), the total duration of turnover curves t_{max} (keeping the temporal resolution constant) (Fig. 4), the number of fitted turnover curves (Fig. 5), and the noise level of turnover curves (Fig. 6). Results are described in more detail in the paragraphs below. For the sake of clarity, in the following paragraphs, we focus on describing the results for two metabolic fluxes of particular interest: $V_{TCA(N)}$ and V_{NT}. We refer to the figures for results regarding the other fitted metabolic fluxes: V_{PC}, $V_{TCA(A)}$, V_X, and V_{OUT}.

The relative SD on metabolic fluxes increased when the number of time points per turnover curve decreased while the duration of experiment was kept constant (t_{max} = 150 min) (Fig. 3). Although the relative SD of all fitted metabolic fluxes increased as the number of data points per curve decreased, some of the fitted fluxes seemed more reliable than others. In this Monte-Carlo simulation carried out with seven turnover curves fitted (Glu C4, C3, C2, Gln C4, C3, C2, and AspC23) and a noise level σ = 0.2 μmol g^{-1}, the relative deviation on $V_{TCA(N)}$ was 10% for 50 experimental points per curve (corresponding to a temporal resolution of 3 min) and increased slightly to 17% for 20 experimental points per curve (corresponding to a temporal resolution of 7.5 min). In contrast, the determination of V_{NT} was less precise. The relative SD on V_{NT} was 45% for 50 data points per curve, and increased sharply in a non-linear fashion when the number of points was decreased, reaching 96% for 30 data points per curve and 670% for 20 points per curve.

A similar simulation was carried out while keeping the temporal resolution constant (5 min), and increasing t_{max} (Fig. 4). The SD on $V_{TCA(N)}$ was 12% for t_{max} = 250 (50 data points per curve) and 15% for t_{max} = 100 min (20 data points per curve). V_{NT} was again less reliable, especially at shorter t_{max}, with a relative SD equal to 41% at t_{max} = 250 min and reaching 96% at t_{max} = 150 min and >3,000% at t_{max} = 100 min. Regardless of the relative precision of $V_{TCA(N)}$ and V_{NT}, this also suggests that fitting turnover curves acquired over a longer time period leads to a more precise determination of metabolic fluxes.

Simulations carried out while varying the number of fitted turnover curves (Fig. 5) also showed that V_{NT} was less reliable than other fluxes. In ^{13}C metabolic modeling studies, the number of fitted turnover curves typically ranges from two curves (fitting glutamate C4 and glutamine C4 turnover only) or three curves (fitting glutamate C4, glutamine C4, and the sum of glutamate and glutamine C3, referred to as Glx C3) to seven curves (fitting turnover curves for glutamate C4, C3, C2, glutamine C4, C3, C2, and AspC23). Monte-Carlo simulations showed again that $V_{TCA(N)}$ was the most reliable flux, with a standard SD decreasing from 10% for seven curves fitted to 20% for three curves fitted. In contrast, the relative SD on V_{NT} was increased from 49% for seven curves fitted to 64% for four curves fitted (Glu C4, C3 and Gln C4, C3) and to 266% for three

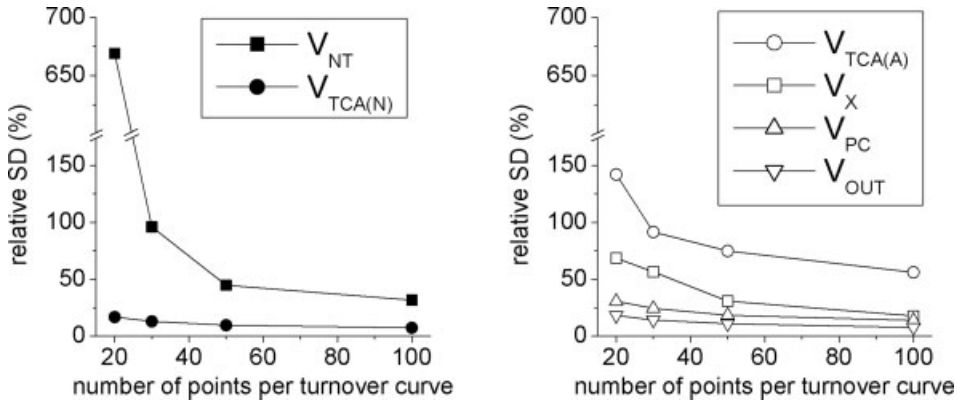

Fig. 3. Relative SD of fitted metabolic fluxes depending on the number of data points per turnover curve. **Left:** Relative SD for $V_{TCA(N)}$ and V_{NT}. **Right:** Relative SD for $V_{TCA(A)}$, V_X, V_{PC}, and V_{OUT}. Note that the SD on V_{NT} increases sharply as the number of data points per curve decreases. This simulation was carried out with seven turnover curves fitted (Glu C4, C3, C2, Gln C4, C3, C2, and AspC23) and a noise level $\sigma = 0.2$ μmol g^{-1}. The total duration of turnover curves was kept constant ($t_{max} = 150$ min).

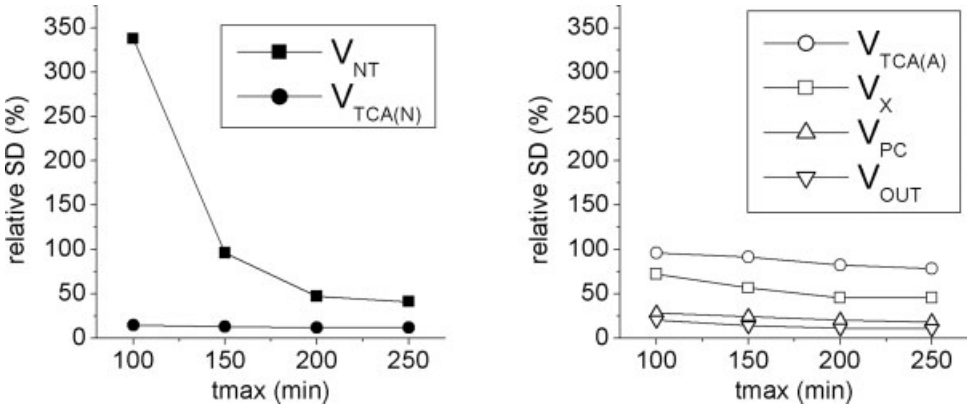

Fig. 4. Relative SD of fitted metabolic fluxes depending on t_{max}. **Left:** Relative SD for $V_{TCA(N)}$ and V_{NT}. **Right:** Relative SD for $V_{TCA(A)}$, V_X, V_{PC}, and V_{OUT}. This simulation was carried out with seven turnover curves fitted (Glu C4, C3, C2, Gln C4, C3, C2, and AspC23) and a noise level $\sigma = 0.2$ μmol g^{-1}. The temporal resolution was kept constant (5 min) so that $t_{max} =$ 100 min corresponded to 20 data points per turnover curve and $t_{max} =$ 250 min corresponded to 50 data points per turnover curve.

curves fitted (Glu C4, Gln C4, and Glx C3). When fitting only two turnover curves (Glu C4 and Gln C4), the relative SD on V_{NT} increased to the very high value of 10,000% (not shown), indicating that this flux could not be determined reliably under these conditions.

Finally, simulations carried out while varying the noise level of turnover curves also indicated that V_{NT} was less reliable than other fluxes, particularly when the noise level increased (Fig. 6). The relative SD on $V_{TCA(N)}$ remained <16% even for a noise level equal to 0.3 μmol g^{-1}, whereas the relative SD on V_{NT} increased sharply in a non-linear fashion as the noise level increased, reaching 45% for $\sigma = 0.2$ μmol g^{-1}, 179% for $\sigma = 0.25$ μmol g^{-1} and more than 5,000% for $\sigma =$ 0.3 μmol g^{-1}.

Results obtained with Monte-Carlo simulations were consistent with sensitivity analysis. We examined the sensitivity of ^{13}C turnover curves for glutamate and glutamine to changes in the value of $V_{TCA(N)}$ or V_{NT} (Fig. 7). Changing the value of $V_{TCA(N)}$ by ±50% resulted in large changes in simulated ^{13}C turnover curves for glutamate C4 and glutamine C4 (Fig. 7, top). In contrast, changing the value of V_{NT} by ±50% resulted in very little change in simulated ^{13}C turnover curves (Fig. 7, bottom), indicating that these curves are not very sensitive to the value of V_{NT}.

Constraining some of the six unknown metabolic fluxes improved the determination of the remaining fitted fluxes (Table I). For example, when fitted seven turnover curves with 20 data points per curve and a noise level $\sigma = 0.2$ μmol.g^{-1}, the relative SD on V_{NT} dropped from 670% with no constrained parameters to 99% when constraining V_X, V_{PC} and $V_{TCA(A)}$ to their nominal value. However, even with these constraints, the relative SD on V_{NT} (99%) remained much higher than the relative SD on $V_{TCA(N)}$ (10 %) and the estimation of the mean value of V_{NT} was biased compared to the nominal value (0.3 μmol g^{-1}min^{-1}).

DISCUSSION

In the present study, we investigated the reliability of two-compartment modeling as it has been carried out

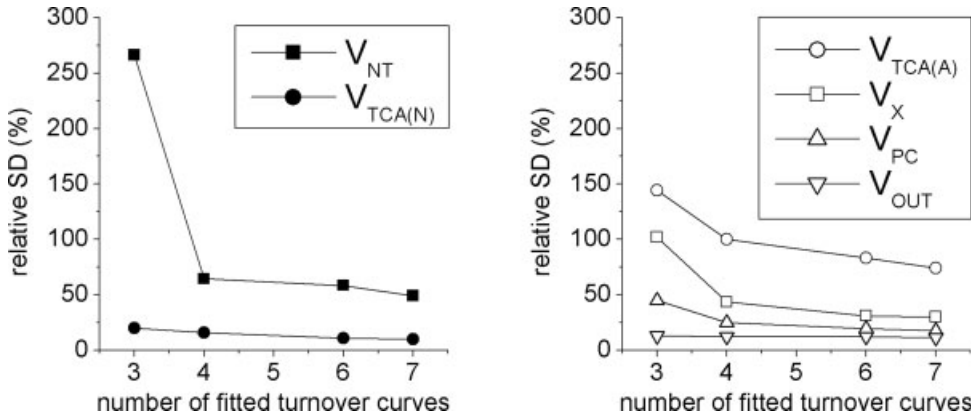

Fig. 5. Relative SD of fitted metabolic fluxes depending the number of turnover curves fitted. **Left:** Relative SD for $V_{TCA(N)}$ and V_{NT}. **Right:** Relative SD for $V_{TCA(A)}$, V_X, V_{PC}, and V_{OUT}. The number of turnover curves fitted corresponded to the following: two curves (Glu C4 and Gln C4), three curves (Glu C4, Gln C4, and Glx C3), four curves (Glu C4, C3 and Gln C4, C3), six curves (Glu C4, C3, C2, and Gln C4, C3, C2), and seven curves (Glu C4, C3, C2, and Gln C4, C3, C2, and Asp23), where Glx C3 is the sum of Glu C3 and Gln C3, and Asp23 is the average of Asp C2 and Asp C3. This simulation was carried out with a noise level $\sigma = 0.2$ μmol g^{-1}, 50 data points per turnover curve and t_{max} =150 min. When fitting only two curves (Glu C4 and Gln C4), the resulting SD on V_{NT} was extremely high (10,000%) and this value is therefore not shown on the graph. Such a high SD suggests that fitting only two curves (Glu C4 and Gln C4) is not sufficient to obtain a reliable measurement of V_{NT}.

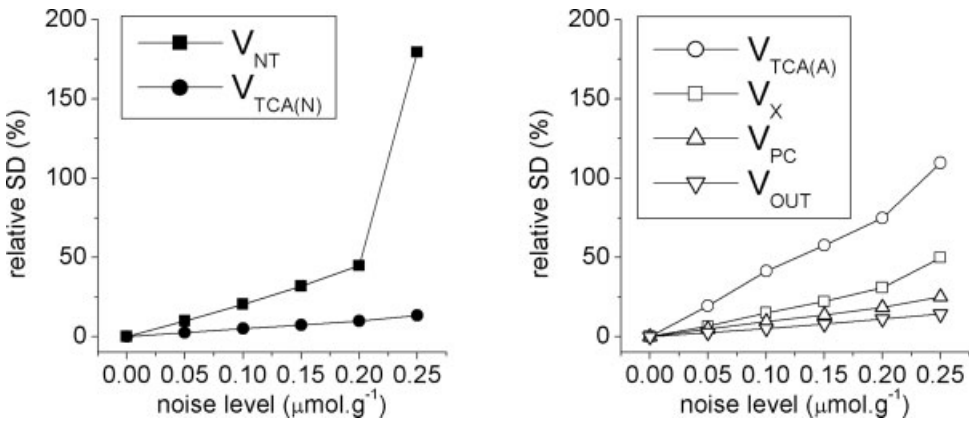

Fig. 6. Relative SD of fitted metabolic fluxes depending on the noise level (noise standard deviation σ in μmol g^{-1}). **Left:** Relative standard deviation for $V_{TCA(N)}$ and V_{NT}. **Right:** Relative SD for $V_{TCA(A)}$, V_X, V_{PC}, and V_{OUT}. This simulation was carried out with seven turnover curves fitted (Glu C4, C3, C2, Gln C4, C3, C2, and AspC23), 50 data points per turnover curve, and $t_{max} = 150$ min.

in the past 10 years to determine compartmentalized neuronal-glial metabolic fluxes. The present study shows that metabolic modeling of ^{13}C positional enrichment curves measured during an infusion of [1-^{13}C] or [1,6-$^{13}C_2$]glucose using a two-compartment neuronal-glial model may not be sufficient to obtain a precise determination of V_{NT}. The error on V_{NT} was generally much higher than the error on $V_{TCA(N)}$ and increased dramatically in a non-linear fashion when experimental conditions became less favorable (lower number of data points per turnover curve, lower total duration of turnover curves, lower signal-to-noise, lower number of turnover curves fitted) as is often the case for in vivo studies. Consistent with these results, ^{13}C turnover curves for glutamate and glutamine were found to be relatively insensitive to the value of V_{NT}.

Reliability of Two-Compartment Modeling Depending on Experimental Conditions

Experimental conditions simulated here are representative of many in vivo studies. Typical in vivo experimental conditions lead to ^{13}C time courses measured with 60–120 min total duration (sometimes longer in animals studies) and a temporal resolution of 5–10 min with a noise SD ranging between 0.1–0.3 μmol g^{-1}. Another experimental aspect to consider is the number of turnover curves fitted. Most studies have used only two turnover curves (glutamate C4 and glutamine C4) or three turnover curves (glutamate C4, glutamine C4, and Glx C3) (de Graaf et al., 2004) to determine V_{NT}. To the best of our knowledge, only two studies in vivo have used six or seven turnover curves (Gruetter et al., 2001; Choi et al., 2002). Our Monte-Carlo simulations suggest that metabolic modeling with two-compart-

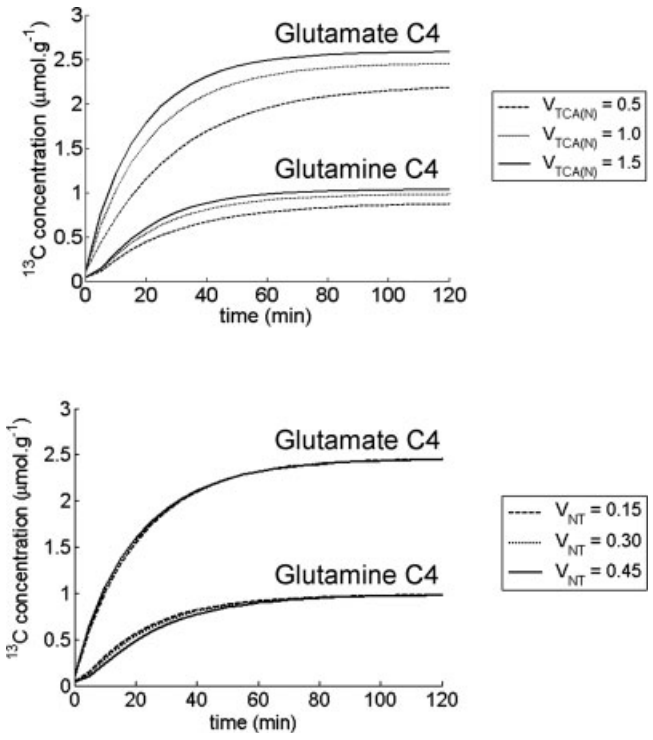

Fig. 7. Sensitivity of ^{13}C turnover curves for glutamate C4 and glutamine C4 to the value of $V_{TCA(N)}$ and V_{NT}. **Top:** ^{13}C turnover curves for glutamate C4 and glutamine C4 when $V_{TCA(N)}$ is varied by ±50% around its nominal value ($V_{TCA(N)}$ = 0.5, 1, and 1.5 µmol g^{-1} min^{-1}). **Bottom:** ^{13}C turnover curves for glutamate C4 and glutamine C4 when V_{NT} is varied by ±50% around its nominal value (V_{NT} = 0.15, 0.3, and 0.45 µmol. g^{-1} min^{-1}).

ment models becomes more reliable when using at least four turnover curves (Glu C4, C3 and Gln C4, C3). The number of curves that can be measured simultaneously largely depends on the NMR detection method and pulse sequence used. For example, direct detection allows separate measurement of Glu C3 and Gln C3, but these two resonances are very difficult to separate with indirect detection methods (Pfeuffer et al., 1999; De Graaf et al., 2003a).

Monte-Carlo simulations reported in the present study suggest that particular caution is warranted when using two-compartment models to fit few turnover curves (for example only two curves Glu C4 and Gln C4). Caution is also warranted when fitting curves with very few points (e.g., time courses obtained cross-sectionally from brain extracts) or with a low signal-to-noise ratio. Constraining some of the free parameters in the model (e.g., constraining V_{PC}, $V_{TCA(A)}$, and V_X, and leaving the other three parameters V_{NT}, $V_{TCA(N)}$ and V_{OUT} as free parameters) may significantly improve the reliability of the fit (Table I), but this requires making assumptions on the constrained metabolic fluxes. Incorrect assumptions may lead to biased estimation of the remaining metabolic fluxes. Furthermore, even with additional constraints, the glutamate-glutamine cycle flux

TABLE I. Standard Deviation on V_{NT} Determined With and Without Constraints on Some of the Other Fitted Parameters*

Parameters fixed	No. of curves	Mean V_{NT}	Absolute SD V_{NT}	Relative SD V_{NT} (%)[a]
None	7	0.56	2.01	670
$V_{TCA(A)}$, V_{PC}	7	0.42	0.52	173
$V_{TCA(A)}$, V_{PC}, V_X	7	0.41	0.30	99
None	3	Unreliable	Unreliable	Unreliable
$V_{TCA(A)}$, V_{PC}	3	0.98	7.88	2,630
$V_{TCA(A)}$, V_{PC}, V_X	3	0.98	2.01	670

*This simulation was carried out with t_{max} = 150 min, 20 data points per turnover curve, and a noise level σ = 0.2 µmol g^{-1}.[a]With respect to nominal value V_{NT} = 0.3 µmol g^{-1} min^{-1}.

V_{NT} remains relatively unreliable, especially when fitting only glutamate C4 and glutamine C4 turnover curves.

In addition to $V_{TCA(N)}$ and V_{NT}, four other metabolic fluxes were estimated in the model. Results of Monte-Carlo simulations showed that the lactate dilution flux V_{OUT} had a precision similar to that of $V_{TCA(N)}$ (10–15% under most simulated experimental conditions). The anaplerotic flux V_{PC} was also relatively reliable with a standard deviation around 20–30% under most simulated experimental conditions. The astrocytic TCA cycle $V_{TCA(A)}$ had a high relative standard deviation (typically 100%) although the absolute error was low, due to low absolute value of this flux in the model (0.1 µmol g^{-1} min^{-1}). The exchange rate V_X between 2-oxoglutarate and glutamate showed a large relative error (~50%), and was therefore much less reliable than $V_{TCA(N)}$, a fact that was already noted in previous studies with one-compartment and two-compartment models (Mason et al., 1992; Gruetter et al., 2001; Choi et al., 2002; Henry et al., 2002).

Insensitivity of ^{13}C Turnover Curves to the Value of V_{NT}

Consistent with Monte-Carlo simulations, we show that glutamate and glutamine ^{13}C positional enrichment curves obtained during an infusion of [1-^{13}C] or [1,6-$^{13}C_2$]glucose are not very sensitive to the value of V_{NT}. This insensitivity of ^{13}C labeling curves to the value of V_{NT} results directly from 1) the relative pool sizes of glutamate and glutamine in glia and neurons, and 2) the fact that most ^{13}C label is taken up by neurons. Therefore, quantitatively, most ^{13}C label flows into the big pool of neuronal glutamate before labeling the smaller pool of glial glutamine. The consequence of this is best understood when considering a simplified version of the two-compartment model (Fig. 8) that assumes that all label flows from glucose into the neuronal glutamate pool, which is in "exchange" with the glial glutamine pool [this model is similar to that used by Sibson et al. (1997, 1998) in the first V_{NT} measurements]. When the neuronal glutamate pool is much larger than the glial glutamine pool ([GLU] >> [GLN] in the simplified model in Fig. 8), simulations indicate that ^{13}C

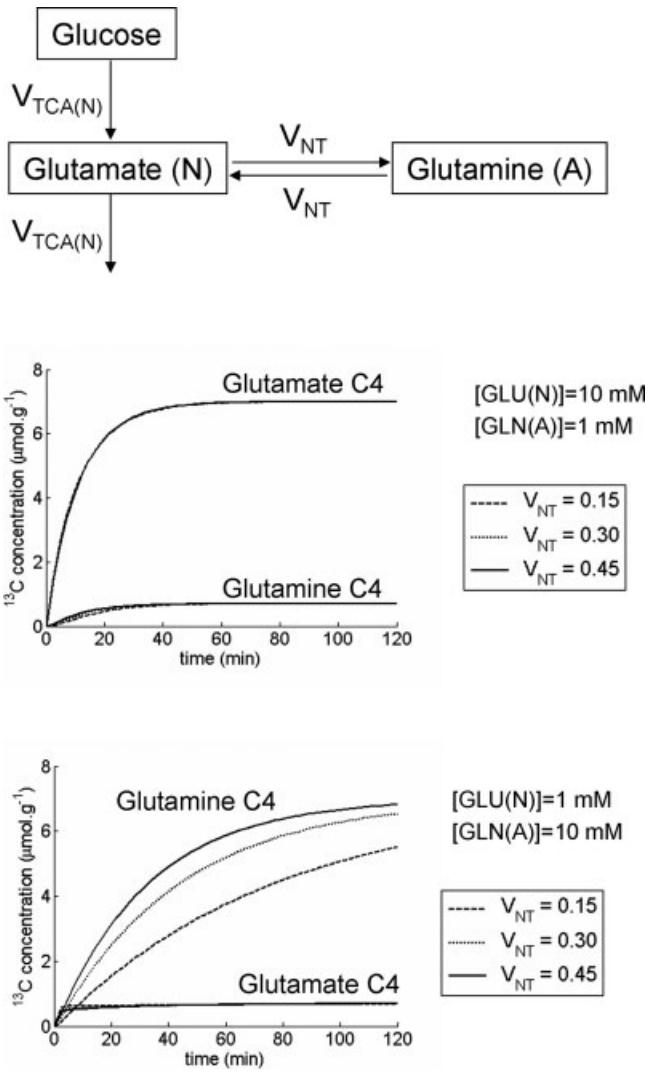

Fig. 8. Illustration of the impact of glutamate and glutamine pool sizes on the ^{13}C positional enrichment time course of glutamate C4 and glutamine C4. **Top:** Simplified version of the two-compartment model in which all ^{13}C label flows from pyruvate to neuronal glutamate, which is in "exchange" with glial glutamine. Although simple, this model reflects the dominant pathway for the flow of ^{13}C label when using [1-^{13}C]glucose or [1,6-$^{13}C_2$]glucose. Most ^{13}C label flows from glucose (or pyruvate) into a big pool (neuronal glutamate), followed by labeling of a smaller pool (glial glutamine). **Middle:** Glutamate C4 and glutamine C4 ^{13}C labeling curves for three different values of V_{NT} (0.15, 0.30, and 0.45 μmol g^{-1} min^{-1}) with [GLU(N)] = 10 mM and [GLN(A)] = 1 mM. The rate of glutamine labeling is nearly independent of V_{NT}. **Bottom:** Glutamate C4 and glutamine C4 ^{13}C labeling curves for three different values of V_{NT} (0.15, 0.30 and 0.45 μmol g^{-1} min^{-1}) with [GLU(N)] = 1 mM and [GLN(A)] = 10 mM. The rate of glutamine labeling depends strongly on the value of V_{NT}.

positional enrichment curves are to a large extent independent of the value of V_{NT} (Fig. 8). In contrast, in the hypothetical case where the glial glutamine pool would be much larger than the neuronal glutamate pool ([GLN] >> [GLU]), simulated ^{13}C positional curves for glutamine become very sensitive to the value of V_{NT} (Fig. 8).

Therefore, the fact the ^{13}C labeling curves are relatively insensitive to value of V_{NT} (when using [1-^{13}C] or [1,6-$^{13}C_2$]glucose as a substrate) is not dependent on particular assumptions used in the two-compartment metabolic model. Rather, it is a consequence of the fact that a large metabolic pool gets labeled more slowly than a small metabolic pool. Therefore, when labeling a small metabolic pool (glial glutamine) from a larger metabolic pool (neuronal glutamate), enrichment curves of the small pool reflect that of the larger precursor pool, with little dependence on the value of the metabolic flux between the two pools. Although the difference in pool sizes is relatively large in the above example (10 mM and 1 mM), additional simulations show that, as long as the precursor pool (e.g., glutamate) is larger than the product pool (e.g., glutamine), labeling of the product pool remains relatively insensitive to the value of the metabolic flux between the two pools (not shown). This illustrates the usefulness of Monte-Carlo simulations and sensitivity analysis to predict how precisely metabolic fluxes can be determined for specific infused substrates, metabolic models, and experimental conditions.

Future Directions to Improve the Reliability of Metabolic Modeling: Acetate

Most dynamic metabolic modeling studies have used [1-^{13}C] or [1,6-$^{13}C_2$]glucose infusion as a substrate. One way to alleviate the uncertainty in metabolic modeling may be to use ^{13}C-labeled substrates that are taken up by a specific compartment. Acetate has been shown to be taken up almost exclusively by astrocytes (Waniewski and Martin, 1998). Because ^{13}C-labeled acetate is taken up only by the glial compartment, the main glial glutamine pool becomes labeled before the large neuronal glutamate pool. Therefore glutamate and glutamine labeling curves are expected to be more sensitive to the value of V_{NT} than with [1-^{13}C] or [1,6-$^{13}C_2$]glucose. A few studies have reported the use of [1-^{13}C]acetate or [2-^{13}C]acetate to study compartmentalized brain metabolism in vivo (Bluml et al., 2002; Lebon et al., 2002; Patel et al., 2005). None of these ^{13}C-acetate studies have attempted dynamic metabolic modeling with a two-compartment neuronal-glial model for quantitative measurement of V_{NT}, however, in part because the kinetics of ^{13}C-acetate uptake and its conversion to acetyl-CoA (in competition with the glycolytic pathway) are not well characterized.

In previous [2-^{13}C]acetate studies, analysis of isotope distribution at isotopic steady-state was used to determine the ratio $V_{NT}/V_{TCA(N)}$ (Lebon et al., 2002). Using this approach, a recent study carried out metabolic modeling (three-compartment model) using data from two separate experiments (Patel et al., 2005). In a first step, [2-^{13}C]acetate was infused to determine the ratio $V_{NT}/V_{TCA(N)}$ using analysis at isotopic steady-state. In a second step (in separate animals), [1,6-$^{13}C_2$]glucose was

infused and the resulting ^{13}C glutamate C4 and glutamine C4 turnover curves were fitted with a two-compartment metabolic model, but using the constrained ratio determined in the first step. Not surprisingly, Monte-Carlo simulations show that the determination of V_{NT} becomes much more reliable when using the additional constraint on the ratio $V_{NT}/V_{TCA(N)}$ (not shown). However, the precision on V_{NT} using this approach is dependent on the precision of the first step (isotopic analysis at isotopic steady-state). A straightforward error calculation on the formula used to calculate the ratio $V_{NT}/V_{TCA(N)}$ (Lebon et al., 2002) shows that, with errors on isotopic enrichment as reported in the same study, the error on V_{NT} is $\sim$75%. Therefore, even though this two-step approach certainly improves the reliability of V_{NT} determination (Patel et al., 2005), it may not be sufficient to yield a very precise measurement of V_{NT}.

One drawback of using [2-^{13}C]acetate as a substrate is that it leads to much lower enrichments in the C2, C3, and C4 resonances of glutamate and C2, C3 resonances of glutamine than enrichments achieved with [1-^{13}C] or [1,6-$^{13}C_2$]glucose infusion, with makes it more difficult to detect signals with sufficient sensitivity in vivo using NMR. In addition, infusion of large amounts of acetate is likely to alter brain physiologic conditions (e.g., increased pyruvate recycling). Nonetheless, we expect that dynamic modeling of turnover curves obtained during [2-^{13}C]acetate infusion may lead to a more robust determination of V_{NT} than when using [1-^{13}C] or [1,6-$^{13}C_2$]glucose.

In another study (Sibson et al., 2001), infusion of [2-^{13}C]glucose also resulted in ^{13}C label being incorporated specifically through the glial compartment via pyruvate carboxylase (metabolism of [2-^{13}C]glucose via pyruvate dehydrogenase complex leads to ^{13}C label being incorporated into glutamate and glutamine C5, which are not detected typically with in vivo NMR detection methods). Metabolic modeling of ^{13}C positional enrichment curves measured during [2-^{13}C]glucose infusion was carried out under hyperammonemic conditions (Sibson et al., 2001). Dynamic metabolic modeling was not possible under normoammonemic conditions in that study, however, due to low signal-to-noise ratio (resulting from the low isotopic enrichment in glutamate and glutamine).

Future Directions to Improve the Reliability of Metabolic Modeling: Dynamic Isotopomer Analysis

Another way to make the metabolic modeling more reliable would be to use the additional information from ^{13}C isotopomers. For example, during infusion of [1-^{13}C] or [1,6-$^{13}C_2$]glucose, the glutamate C4 resonance (GluC4total) appears as the superposition of a singlet (GluC4S corresponding to glutamate labeled at the C4 position, but not at the C5 or C3 positions) and a doublet (GluCD43 corresponding to glutamate labeled both at C4 and C3 positions). We have shown recently that dynamic isotopomer time courses can be measured in the brain in vivo (Henry et al., 2003a,b). Jeffrey et al. (1999) have shown in the heart that using this additional information from isotopomers leads to improved determination of V_{TCA}. In the brain, however, current metabolic models used to analyze ^{13}C turnover curves in the brain consider only the total amount of ^{13}C label at each carbon position (^{13}C positional enrichment), but do not take advantage of the additional information available from ^{13}C-^{13}C multiplets. For example, positional models fit the ^{13}C positional enrichment curve for glutamate C4 (GluC4total), but does not take advantage of the additional information from the singlet GluC4S and the doublet GluC4D43. We are developing currently a new metabolic model to fit additional ^{13}C turnover curves corresponding to multiply labeled ^{13}C-^{13}C isotopomers.

Usefulness of Monte-Carlo Simulations to Evaluate the Precision of Metabolic Models

As metabolic models become more complex, with a higher number of free parameters and more assumptions, it is useful to increasingly evaluate the reliability of such models. Monte-Carlo simulations are a widely accepted mathematical procedure to evaluate the reliability of models with respect to noise in experimental data, and we expect that they will become an indispensable component of ^{13}C metabolic modeling studies. Note that the present study only addressed the precision of metabolic fluxes using existing two-compartment metabolic models. Although we used the most up to date metabolic model in use currently, we did not attempt to verify whether all assumptions in this model are correct. Our question was simply: given existing two-compartment models, what precision can be expected on the determination of metabolic fluxes?

Metabolic models will undoubtedly still be refined with time as more prior knowledge becomes available. For example, current models do not consider the possibility of net glutamate oxidation into the astrocytic TCA cycle. Studies by McKenna et al. (1996) show that glutamate oxidation occurs in astrocytes in culture. It is unclear whether net glutamate oxidation occurs in vivo. Extracellular glutamate concentration is normally very low, but it does increase to high levels for brief periods during excitatory neurotransmission (Matsui et al., 2005). Note that if there is net glutamate oxidation (net glutamate influx into TCA cycle), then there should be net efflux of carbons somewhere else in the TCA cycle. One possible mechanism for this is pyruvate recycling. There is evidence, however, that pyruvate recycling is very small in the brain in vivo when infusing glucose. This is because infusion of [1,6-$^{13}C_2$]glucose does not result in significant labeling of glutamate and glutamine C5 even after several hours of infusion (Gruetter et al., 2003b). If there was significant pyruvate recycling, glutamate and glutamine C5 would become labeled, which was not the case. In contrast, a high rate of pyruvate

recycling has been reported during acetate infusion (Cerdan et al., 1990). We also observed that, when infusing [2-^{13}C]acetate, glutamate and glutamine C5 become highly labeled, which suggests a high rate of pyruvate recycling under these conditions (not shown). In addition to pyruvate recycling, another possibility for loss of TCA cycle intermediates is direct efflux of glutamine. We expect that future work will address the possibility of net glutamate oxidation in vivo.

Our finding that V_{NT} is relatively unreliable may seem surprising in view of the significant number of ^{13}C studies carried out using [1-^{13}C]glucose or [1,6-$^{13}C_2$]glucose infusion and two-compartment models to measure V_{NT} in the past decade (Sibson et al., 1997, 1998; Shen et al., 1999; Gruetter et al., 2001; Choi et al., 2002; de Graaf et al., 2004; Oz et al., 2004; Patel et al., 2004, 2005; Yang and Shen, 2005). It is worth noting, however, that one study reported a very high standard deviation on V_{NT} (Chhina et al., 2001), which is consistent with our Monte-Carlo simulations. We suggest several possibilities to explain why the V_{NT} flux seemed more reliable in many studies than would be expected based on Monte-Carlo simulations. First, the fitting algorithm may stop at a local minimum, so that the fitted values obtained after least-square minimization do not correspond to the best fit. One way to circumvent this problem is to repeat the fit with very different initial conditions and to verify that fitted parameter values do not depend on initial conditions. Another explanation for the apparent reliability of V_{NT} in previous studies is that the investigator may introduce some "prior knowledge" by expecting "reasonable" values for metabolic fluxes. For example, the investigator may expect $0 < V_{NT} < V_{TCA(N)}$ (even if this constraint is not implemented explicitly in the fitting algorithm, the investigator may be tempted to repeat the fit with slightly different conditions if the fitted value of V_{NT} is "unreasonable"). With such a constraint, if V_{NT} is so unreliable that the values of V_{NT} are evenly spread in the interval [0; $V_{TCA(N)}$], then on average the determination of V_{NT} is expected to yield $V_{NT} = 0.5 \times V_{TCA(N)}$. This could potentially explain the apparent correlation between V_{NT} and $V_{TCA(N)}$ in previous studies. Finally, uncertainty on fitted parameters may be underestimated by the software. Most fitting software give an estimate of the uncertainty for each fitted parameter based on the fitting algorithm itself (calculated from inversion matrix). However, this determination is based on specific assumptions to calculate so-called asymptotic or approximate standard errors. These assumptions are most likely not verified when fitting "noisy" in vivo data, leading to an underestimation of the true error. Monte-Carlo simulations avoid this problem and are considered the "gold standard" for determination of uncertainties with non-linear models.

CONCLUSION

We conclude that ^{13}C turnover curves for glutamate and glutamine obtained during [1-^{13}C] or [1,6-$^{13}C_2$]glucose infusion are much more sensitive to the value of neuronal TCA cycle rate $V_{TCA(N)}$ than to the value of the glutamate-glutamine cycle rate V_{NT}. As a result, metabolic modeling of ^{13}C turnover curves using two-compartment neuronal-glial metabolic models yields relatively precise estimates of $V_{TCA(N)}$, whereas the determination of V_{NT} is relatively unreliable under experimental conditions typical of in vivo studies. Our study underscores the importance of evaluating the reliability of metabolic modeling under experimental conditions specific for each study. We suggest that Monte-Carlo simulations become a standard component of any metabolic modeling study to evaluate the degree of confidence in each fitted metabolic flux in the model.

ACKNOWLEDGMENTS

This work was supported by NIH Grants R01NS38672 (P.G.H.), P41RR08079 (K.U.), P30NS057091 (K.U.), the Keck Foundation and the MIND institute.

REFERENCES

Bluml S, Moreno-Torres A, Shic F, Nguy CH, Ross BD. 2002. Tricarboxylic acid cycle of glia in the in vivo human brain. NMR Biomed 15:1–5.

Cerdan S, Kunnecke B, Seelig J. 1990. Cerebral metabolism of [1,2-$^{13}C_2$]acetate as detected by in vivo and in vitro ^{13}C NMR. J Biol Chem 265:12916–12926.

Chance MC, Seeholzer SH, Kobayashi K, Williamson JR. 1983. Mathematical analysis of isotope labeling in the citric acid cycle with applications to ^{13}C NMR studies in perfused rat hearts. J Biol Chem 258:13785–13794.

Chhina N, Kuestermann E, Halliday J, Simpson LJ, Macdonald IA, Bachelard HS, Morris PG. 2001. Measurement of human tricarboxylic acid cycle rates during visual activation by (13)C magnetic resonance spectroscopy. J Neurosci Res 66:737–746.

Choi IY, Lei HX, Gruetter R. 2002. Effect of deep pentobarbital anesthesia on neurotransmitter metabolism in vivo: on the correlation of total glucose consumption with glutamatergic action. J Cereb Blood Flow Metab 22:1343–1351.

de Graaf RA, Brown PB, Mason GF, Rothman DL, Behar KL. 2003a. Detection of [1,6-$^{13}C_2$]-glucose metabolism in rat brain by in vivo ^{1}H-[^{13}C]-NMR spectroscopy. Magn Reson Med 49:37–46.

de Graaf RA, Mason GF, Patel AB, Behar KL, Rothman DL. 2003b. In vivo ^{1}H-[^{13}C]-NMR spectroscopy of cerebral metabolism. NMR Biomed 16:339–357.

de Graaf RA, Mason GF, Patel AB, Rothman DL, Behar KL. 2004. Regional glucose metabolism and glutamatergic neurotransmission in rat brain in vivo. Proc Natl Acad Sci USA 101:12700–12705.

Garcia-Espinosa MA, Rodrigues TB, Sierra A, Benito M, Fonseca C, Gray HL, Bartnik BL, Garcia-Martin ML, Ballesteros P, Cerdan S. 2004. Cerebral glucose metabolism and the glutamine cycle as detected by in vivo and in vitro 13C NMR spectroscopy. Neurochem Int 45:297–303.

Gruetter R. 2002. In vivo ^{13}C NMR studies of compartmentalized cerebral carbohydrate metabolism. Neurochem Int 41:143–154.

Gruetter R, Adriany G, Choi I-Y, Henry P-G, Lei H-X, Oz G. 2003a. Localized in vivo ^{13}C NMR spectroscopy of the brain. NMR Biomed 16:313–338.

Gruetter R, Adriany G, Choi IY, Henry PG, Lei H, Oz G. 2003b. Localized in vivo 13C NMR spectroscopy of the brain. NMR Biomed 16:313–338.

Gruetter R, Novotny EJ, Boulware SD, Mason GF, Rothman DL, Shulman GI, Prichard JW, Shulman RG. 1994. Localized ^{13}C NMR spectroscopy in the human brain of amino acid labeling from D-[1-^{13}C]glucose. J Neurochem 63:1377–1385.

Gruetter R, Seaquist ER, Kim S, Ugurbil K. 1998. Localized in vivo ^{13}C-NMR of glutamate metabolism in the human brain: initial results at 4 Tesla. Dev Neurosci 20:380–388.

Gruetter R, Seaquist ER, Ugurbil K. 2001. A mathematical model of compartmentalized neurotransmitter metabolism in the human brain. Am J Physiol 281:E100–E112.

Henry P-G, Oz G, Provencher S, Gruetter R. 2003a. Toward dynamic isotopomer analysis in the rat brain in vivo: automatic quantitation of ^{13}C NMR spectra using LCModel. NMR Biomed 16:400–412.

Henry P-G, Tkac I, Gruetter R. 2003b. ^{1}H-localized broadband ^{13}C NMR spectroscopy of the rat brain in vivo at 9.4 Tesla. Magn Reson Med 50:684–692.

Henry PG, Adriany G, Deelchand D, Gruetter R, Marjanska M, Oz G, Seaquist ER, Shestov A, Ugurbil K. 2006. In vivo 13C NMR spectroscopy and metabolic modeling in the brain: a practical perspective. Magn Reson Imaging 24:527–539.

Henry PG, Lebon V, Vaufrey F, Brouillet E, Hantraye P, Bloch G. 2002. Decreased TCA cycle rate in the rat brain after acute 3-NP treatment measured by in vivo 1H-[13C] NMR spectroscopy. J Neurochem 82:857–866.

Jeffrey FM, Reshetov A, Storey CJ, Carvalho RA, Sherry AD, Malloy CR. 1999. Use of a single (13)C NMR resonance of glutamate for measuring oxygen consumption in tissue. Am J Physiol 277:E1111–1121.

Lebon V, Petersen KF, Cline GW, Shen J, Mason GF, Dufour S, Behar KL, Shulman GI, Rothman DL. 2002. Astroglial contribution to brain energy metabolism in humans revealed by ^{13}C nuclear magnetic resonance spectroscopy: elucidation of the dominant pathway for neurotransmitter glutamate repletion and measurement of astrocytic oxidative metabolism. J Neurosci 22:1523–1531.

Mason GF, Behar KL, Rothman DL, Shulman RG. 1992. NMR determination of intracerebral glucose concentration and transport kinetics in rat brain. J Cereb Blood Flow Metab 12:448–455.

Mason GF, Gruetter R, Rothman DL, Behar KL, Shulman RG, Novotny EJ. 1995. Simultaneous determination of the rates of the TCA cycle, glucose utilization, α-ketoglutarate/glutamate exchange, and glutamine synthesis in human brain by NMR. J Cereb Blood Flow Metab 15:12–25.

Matsui K, Jahr CE, Rubio ME. 2005. High-concentration rapid transients of glutamate mediate neural-glial communication via ectopic release. J Neurosci 25:7538–7547.

McKenna MC, Sonnewald U, Huang X, Stevenson J, Zielke HR. 1996. Exogenous glutamate concentration regulates the metabolic fate of glutamate in astrocytes. J Neurochem 66:386–393.

Ottersen OP, Zhang N, Walberg F. 1992. Metabolic compartmentation of glutamate and glutamine: morphological evidence obtained by quantitative immunocytochemistry in rat cerebellum. Neuroscience 46:519–534.

Oz G, Berkich DA, Henry PG, Xu Y, LaNoue K, Hutson SM, Gruetter R. 2004. Neuroglial metabolism in the awake rat brain: CO_2 fixation increases with brain activity. J Neurosci 24:11273–11279.

Patel AB, de Graaf RA, Mason GF, Kanamatsu T, Rothman DL, Shulman RG, Behar KL. 2004. Glutamatergic neurotransmission and neuronal glucose oxidation are coupled during intense neuronal activation. J Cereb Blood Flow Metab 24:972–985.

Patel AB, de Graaf RA, Mason GF, Rothman DL, Shulman RG, Behar KL. 2005. The contribution of GABA to glutamate/glutamine cycling and energy metabolism in the rat cortex in vivo. Proc Natl Acad Sci USA 102:5588–5593.

Pfeuffer J, Tkac I, Choi I-Y, Merkle H, Ugurbil K, Garwood M, Gruetter R. 1999. Localized in vivo ^{1}H NMR detection of neurotransmitter labeling in rat brain during infusion of [1-^{13}C] D-glucose. Magn Reson Med 41:1077–1083.

Rothman DL, Behar KL, Hyder F, Shulman RG. 2003. In vivo NMR studies of the glutamate neurotransmitter flux and neuroenergetics: implications for brain function. Annu Rev Physiol 65:401–427.

Shen J. 2006. 13C magnetic resonance spectroscopy studies of alterations in glutamate neurotransmission. Biol Psychiatry 59:883–887.

Shen J, Petersen KF, Behar KL, Brown P, Nixon TW, Mason GF, Petroff OAC, Shulman GI, Shulman RG, Rothman DL. 1999. Determination of the rate of the glutamate/glutamine cycle in the human brain by in vivo ^{13}C NMR. Proc Natl Acad Sci USA 96:8235–8240.

Sibson NR, Dhankhar A, Mason GF, Behar KL, Rothman DL, Shulman RG. 1997. In vivo ^{13}C NMR measurements of cerebral glutamine synthesis as evidence for glutamate-glutamine cycling. Proc Natl Acad Sci USA 94:2699–2704.

Sibson NR, Dhankhar A, Mason GF, Rothman DL, Behar KL, Shulman RG. 1998. Stoichiometric coupling of brain metabolism and glutamatergic neuronal activity. Proc Natl Acad Sci USA 95:316–321.

Sibson NR, Mason GF, Shen J, Cline GW, Herskovits AZ, Wall JE, Behar KL, Rothman DL, Shulman RG. 2001. In vivo ^{13}C NMR measurement of neurotransmitter glutamate cycling, anaplerosis and TCA cycle flux in rat brain during [2-^{13}C]glucose infusion. J Neurochem 76:975–989.

Waniewski RA, Martin DL. 1998. Preferential utilization of acetate by astrocytes is attributable to transport. J Neurosci 18:5225–5233.

Yang J, Shen J. 2005. In vivo evidence for reduced cortical glutamate-glutamine cycling in rats treated with the antidepressant/antipanic drug phenelzine. Neuroscience 135:927–937.